Circular Permutation of a WW Domain: Folding still occurs after Excising the Turn of the Folding-Nucleating Hairpin

Brandon L. Kier, Jordan M. Anderson & Niels H. Andersen, University of Washington, Seattle, WA

SUPPORTING FIGURES, tables, and text

Table S1: A complete list of peptides investigated in this study, with names, sequences, melting temperatures, and justification:

Name	Sequence. (Capping Trps: Blue. Core Trp: Red.)	T_M (°C)
WW Domains		
WW **st**34	KLPPG**W**EKR**W**DRGSGR**W**FYFNRITGKRQFERPSD	94
full-length positive control		
WW **st**29	---KG**W**EKR**W**DRGSGR**W**FYFNRITGKRQFERP--	74
full-length standard-topology low-melting enough for lineshape studies		
WW **cp**34	R**W**FYFNRITGKRQFERPSDRGSGKLPPG**W**EKR**W**D	63
initial test of circular permutation		
WW **cp**34 VK	R**W**FYFNRITGKRQFERPSDRGSGKLVKG**W**EKR**W**D	59
circular permutant with prolines removed, to remove spurious NMR peaks		
WW **cp**29	R**W**FYFNRITGKRQFERPK--G---LVKG**W**EKR**W**D	53
shorter circular permutant; lower-melting and no spurious NMR peaks		
Fragment Peptides: Hairpin 1		
stHP1*wt*	RWEKRMSRSSGRVYYFNS	<<0
simple excision of the first hairpin of wild-type WW Pin1		
stHP1	RWEKR**W**DRGSGR**W**FYFND	60
optimized WW hairpin 1; vast improvement over wild-type		
stHP1 PATG	RWEKR**W**NPATGR**W**FYFND	77
further optimization of the turn of WW hairpin 1; faster-folding		
cpHP1*wt*	RVYYFNSRSSGRWEKRMS	<<0
excision plus circular permutation of the first hairpin of wt WW Pin1		
cpHP1	R**W**FYFNDRGSGRWEKR**W**D	34
circular permutation of the optimized WW hairpin 1		
cpHP1 PATG	R**W**FYFNDPATGKWEKR**W**D	49
further optimized (better turn) circular permutant of hairpin 1; faster		
cpHP1 pG	R**W**FYFNI-pG-KWEKR**W**D	65
further optimized (better turn) circular permutant of hairpin 1		
Beta-Loop-Beta: Long Loop Peptides		
blb30	R**W**ITVTIGGGGKKGGGGKKGGGGKKIRV**W**E	30
testing feasibility of beta cap assembly with long contact order		
blb36	R**W**ITVTIGGGGKKGGGGKKGGGGKKGGGGKKIRV**W**E	6
testing feasibility of beta cap assembly with longer contact order		
blb16	R**W**ITVTIGGKKIRV**W**E	>85
positive control for the **blb** series; two residue loop.		

Fig. S1. A (top panel), **st**HP1*wt* and **cp**HP1*wt* (native hairpin & its circular permutant), **st**HP1 and **cp**HP1 (optimized hairpin & its circular permutant) compared to wild-type WW Pin1 (WW **st**34*wt*) over the strand residues of the first hairpin. **B** (middle panel), **st**HP1 and its more stable turn mutant, **st**HP1-PATG compared to WW **st**29. **C** (lower panel), **cp**HP1 and two stabilizing turn mutants PATG and pG) compared to WW **cp**29 over the same residues. The pattern of H_N and Hα CSDs (chemical shift deviations) are consistent with expectations for hairpin folds. (1-3)

Fig. S2A. CD melts showing the loss of both the exciton couplet and the positive peak at ca. 196 nm due to the associated β-strands of two hairpins (**st**HP1 left, and **cp**HP1 right).

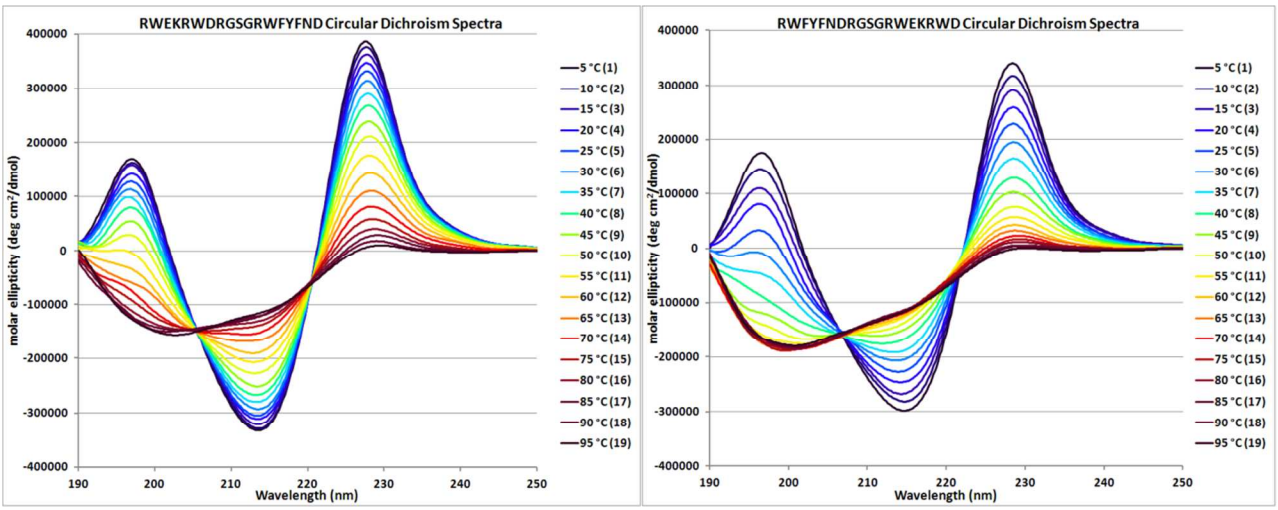

stHP1 **cp**HP1

Fig. S2B. CD melts as $[\theta]_{228}$ versus temperature for the five WW-related hairpin fragments investigated in this study. (From top to bottom: **st**HP1 orange, **cp**HP1 blue, **st**HP1-PATG yellow, **cp**HP1-PATG teal, **cp**HP1-pG magenta.)

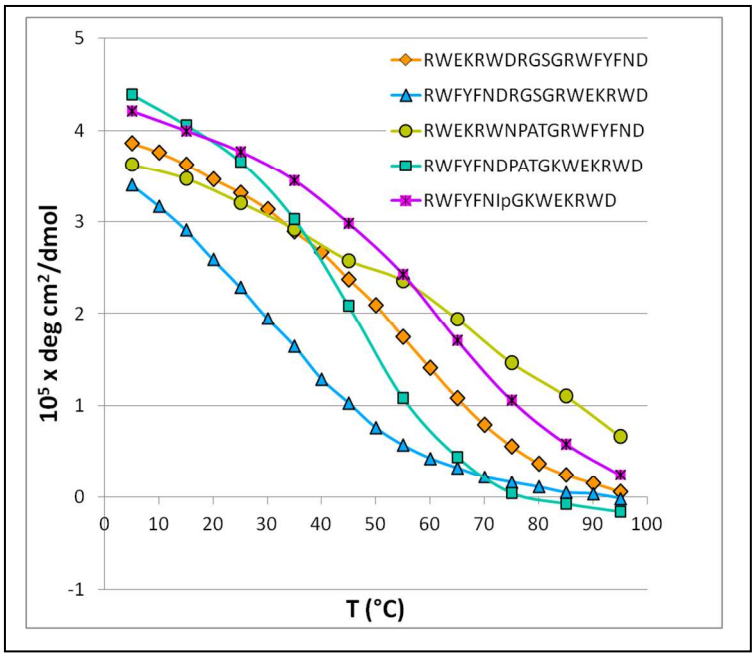

Fig. S3. 1D proton NMR data collected in D_2O medium at 310K showing the linewidth differences between the WW domains WW **st**29 (**st**andard **t**opology) and WW **cp**29 (the **c**ircular **p**ermutant). The less upfield shifted (but broader) Trp Hε3 and Hζ3 signals for the permuted sequence reflect an increased population of the unfolded state and a slower folding rate, respectively.

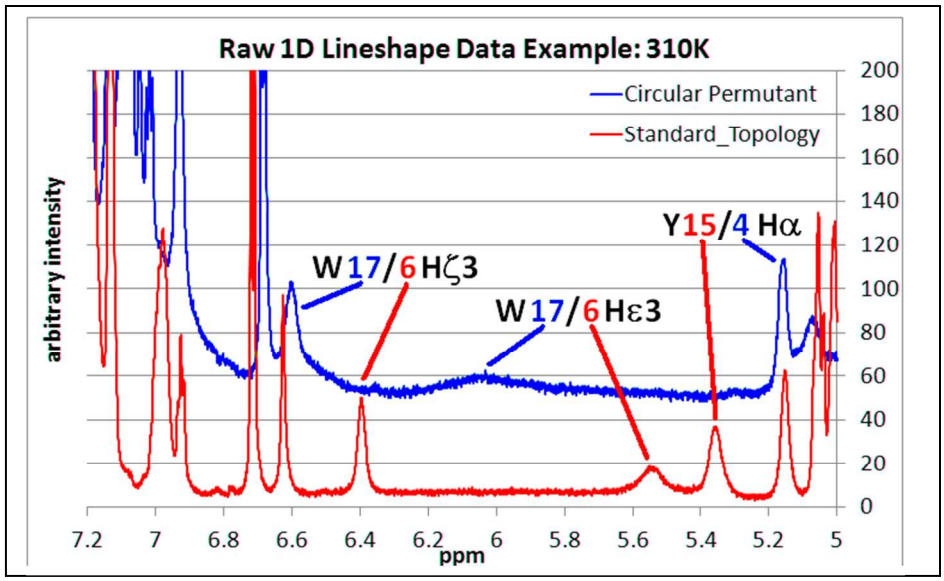

Similar effects are observed for the hairpin models. The method used to extract the exchange broadening term is illustrated in Fig. 2 in the main text.

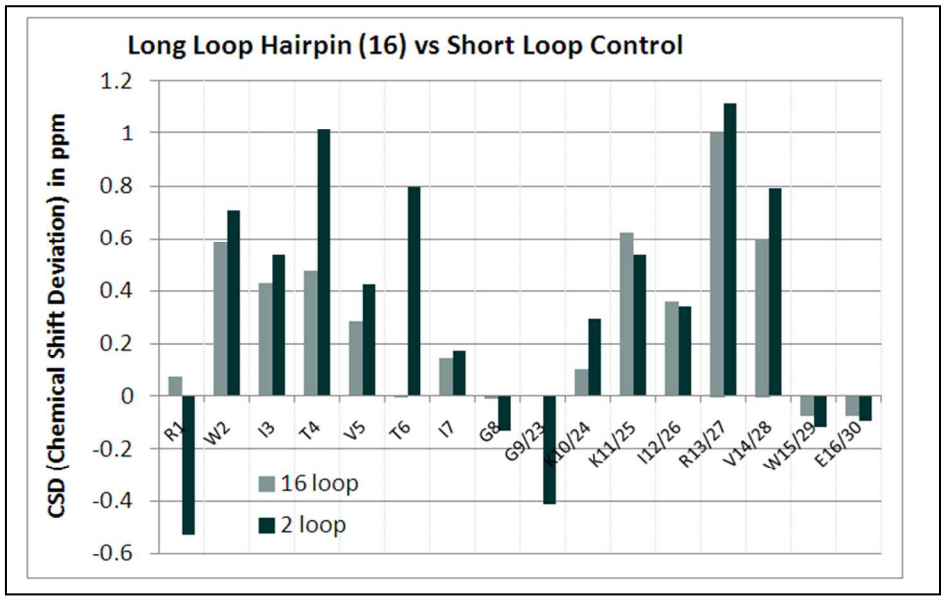

Fig. S4. A chemical shift comparison (as CSDs) of long loop RWITVTI(GGGGKK)$_3$IRVWE (**blb**30, loop length: 16) with RWITVTI-GG-KKIRVWE (**blb**16, loop length: 2) which has $\chi_F > 0.96$ based on its CD and NMR melt.

Alternate loop structures within the folded ensemble.

The NMR spectra of WW **cp**34 had alternate sets of resonances for many proton sites (Fig. S5) indicating the presence of at least one other minor folded isomer. We attributed this to cis/trans backbone isomers about the prolines in the loop and set about eliminating this complication by loop optimization and truncation as shown below.

RW-FYFNRITGKRQFERP - loop - WEKR-WD

WW **cp**34	loop	=	SDRGSGKLPPG
WW **cp**34(P26V,P27K)	loop	=	SDRGSGKLVKG
WW **cp**29	loop	=	KGLVKG

The replacement of the PP unit in the linking loop with VK had a very modest impact on stability, and reduced (though curiously, did not completely eliminate) the presumed cis/trans isomer complication. (Fig. S5, bottom). We were able to reduce the loop length by 5-residues and retain fold formation. At 29 residues, the chain length of WW **cp**29 one residue less than that of the starting WT topology.

Fig. S5. Illustrating additional peaks that are present due to an additional folded species in slow exchange. Both panels are of a circularly permuted WW domain. The top panel is WW **cp**34 which has an SDRGSGKLPPG sequence in the loop connecting two β strands. In the case of WW **cp**34 (P26VP27K), those two prolines were replaced by a Val-Lys unit. Both panels show the Hε1 signals for the three Trp residues.

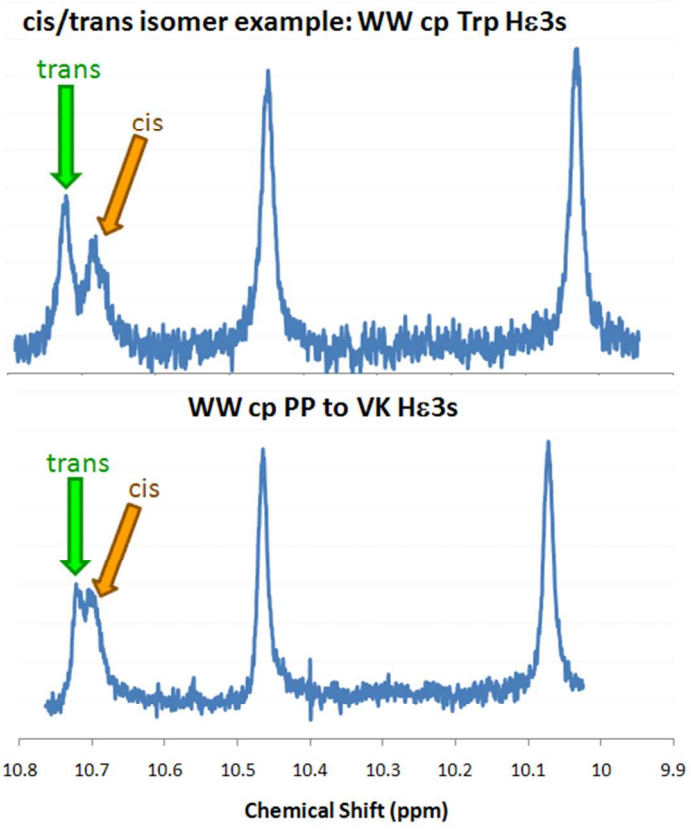

The minor isomer signal is labeled “cis” in each case. There are also minor peaks, typically only partially resolved, for other loop residues and other sites in Trp6. Additional coonectivites cannot be traced in the NOESY. The “cis” peaks are broader, and integrate to almost 60% of “trans”. There is no clear NOE evidence for cis-proline (e.g., no obvious i/i+1 Hα to Hα peak) so this “cis” peak could be some other type of slow-exchanging alternate conformer. Though slow & specific oligomerization is unlikely, it would likely produce a set of alternate peaks localized at the interface, and would not be incompatible with this data.

This set of alternate peaks is only observed for the long-loop circular permutants, and is independent of pH. No extra peaks are observed for WW **cp**29.

Chemical Shift Comparisons, wild type topology versus circular permutants.

Fig. S6A. The proton chemical shift comparison for WW **cp**29 and the wild-type WW Pin1 (**st**34*wt*)

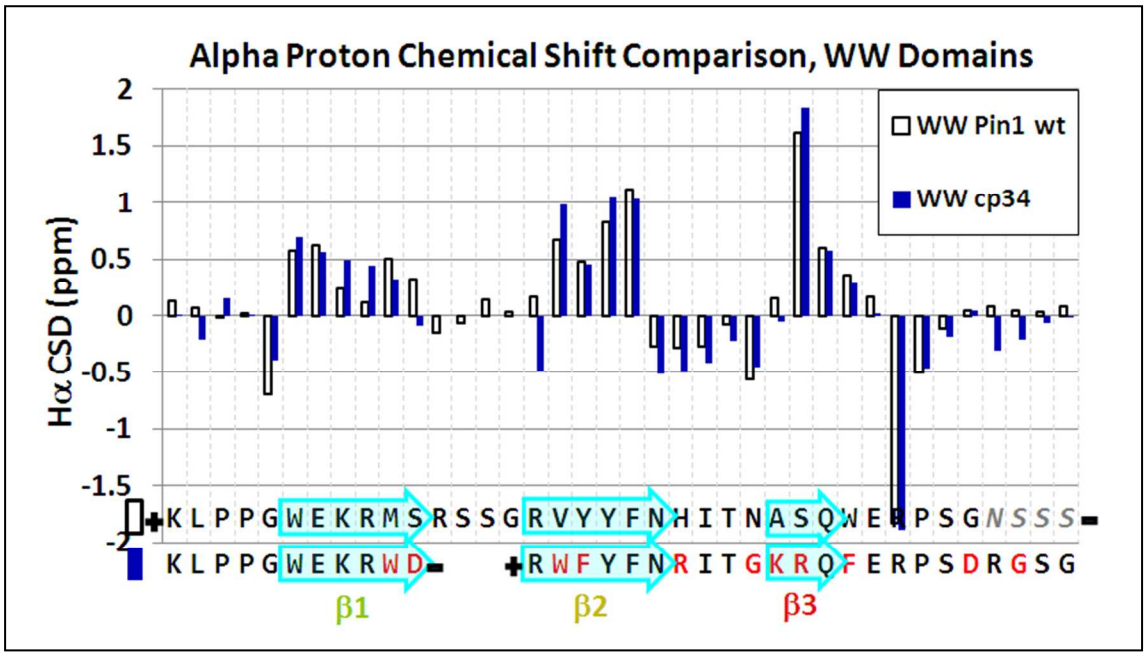

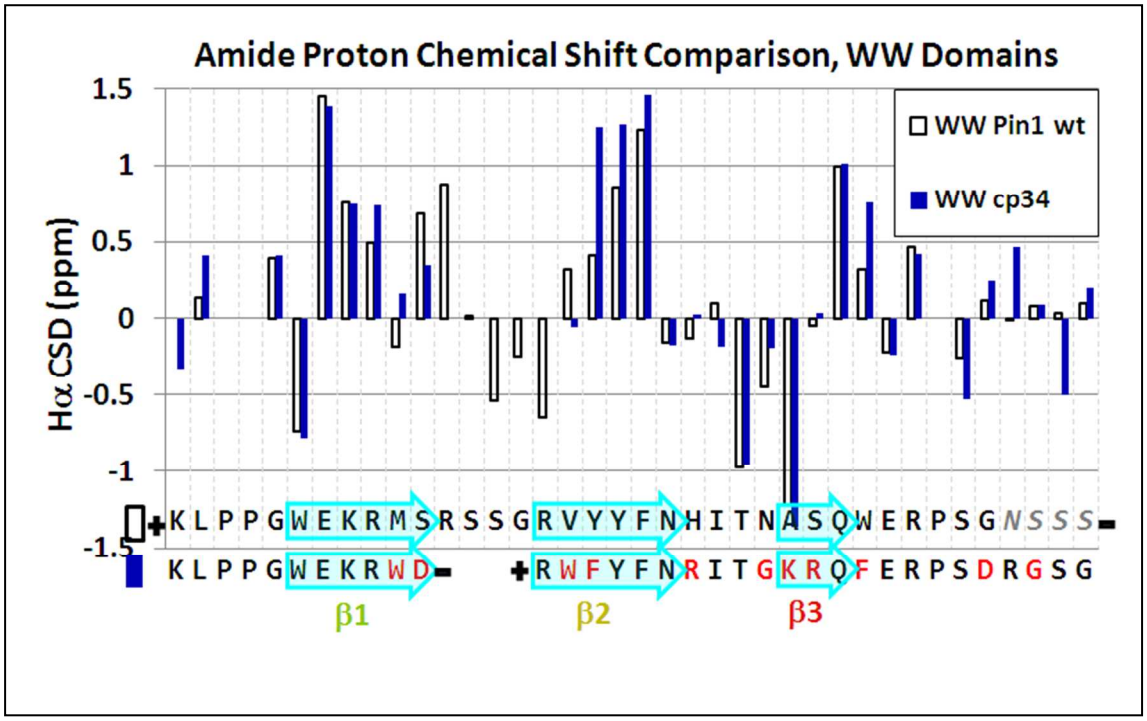

Fig. S6B. Proton chemical shift comparisons (as CSDs) for three sequences with the same residues throughout the core WW fold region: the hyperstable WW **st**34, its truncated variant WW **st**29, and the circular permutant WW **cp**29.

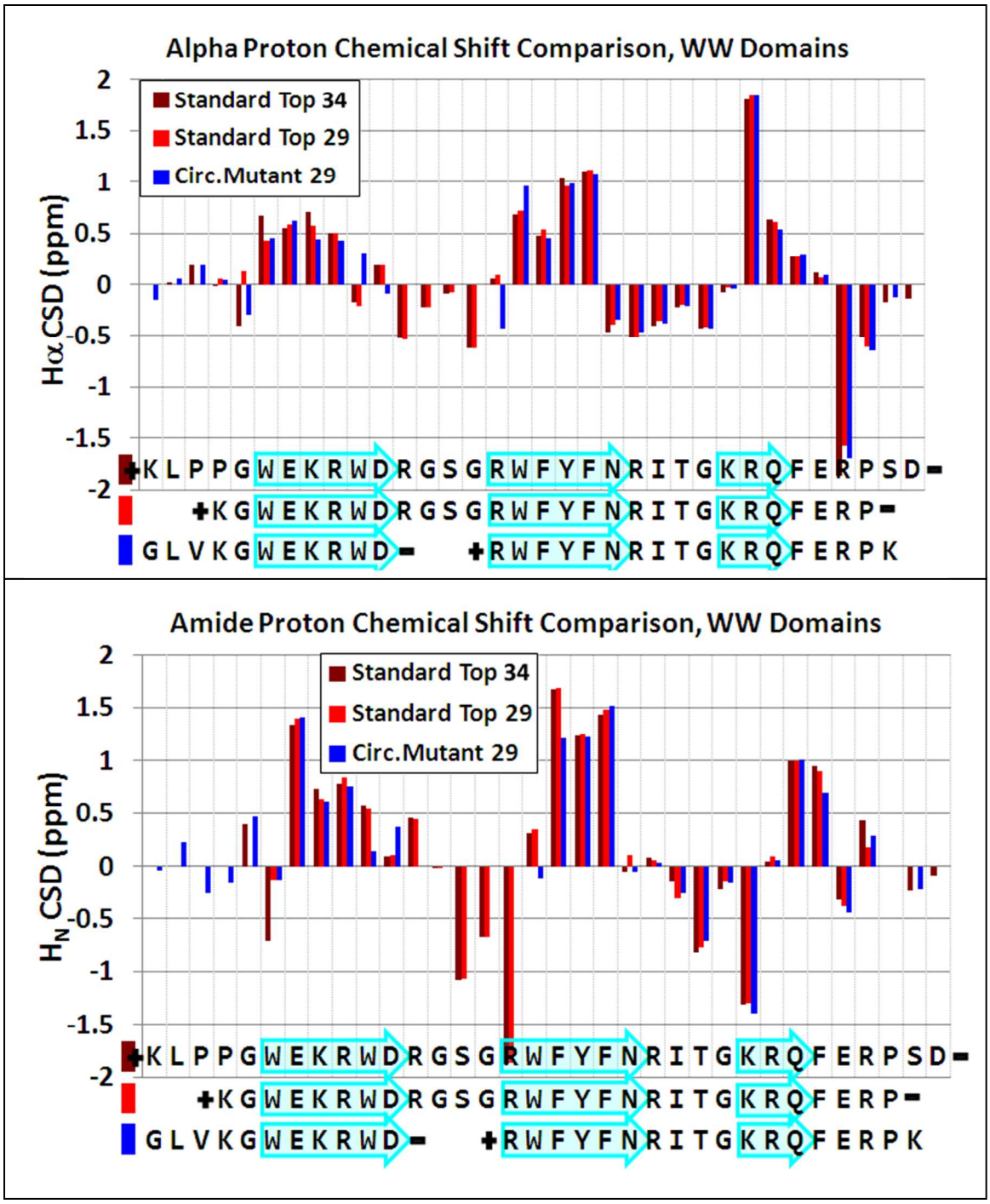

Better CSD correspondence was observed between the circular permutants and the mutated (hyperstable) Pin1 sequence, vs. the circular permutants and wild-type Pin1. This is an expected result of higher sequence identity, and allows for more a more precise analysis of the effect of circular permutation.

Fig. S7. Fully folded CSD versus temperature plots for the probes used in dynamics analysis: taken from the hyperstable standard topology construct (WW **st**34) at temperatures well below its melting transition (Tm = 94 °C).

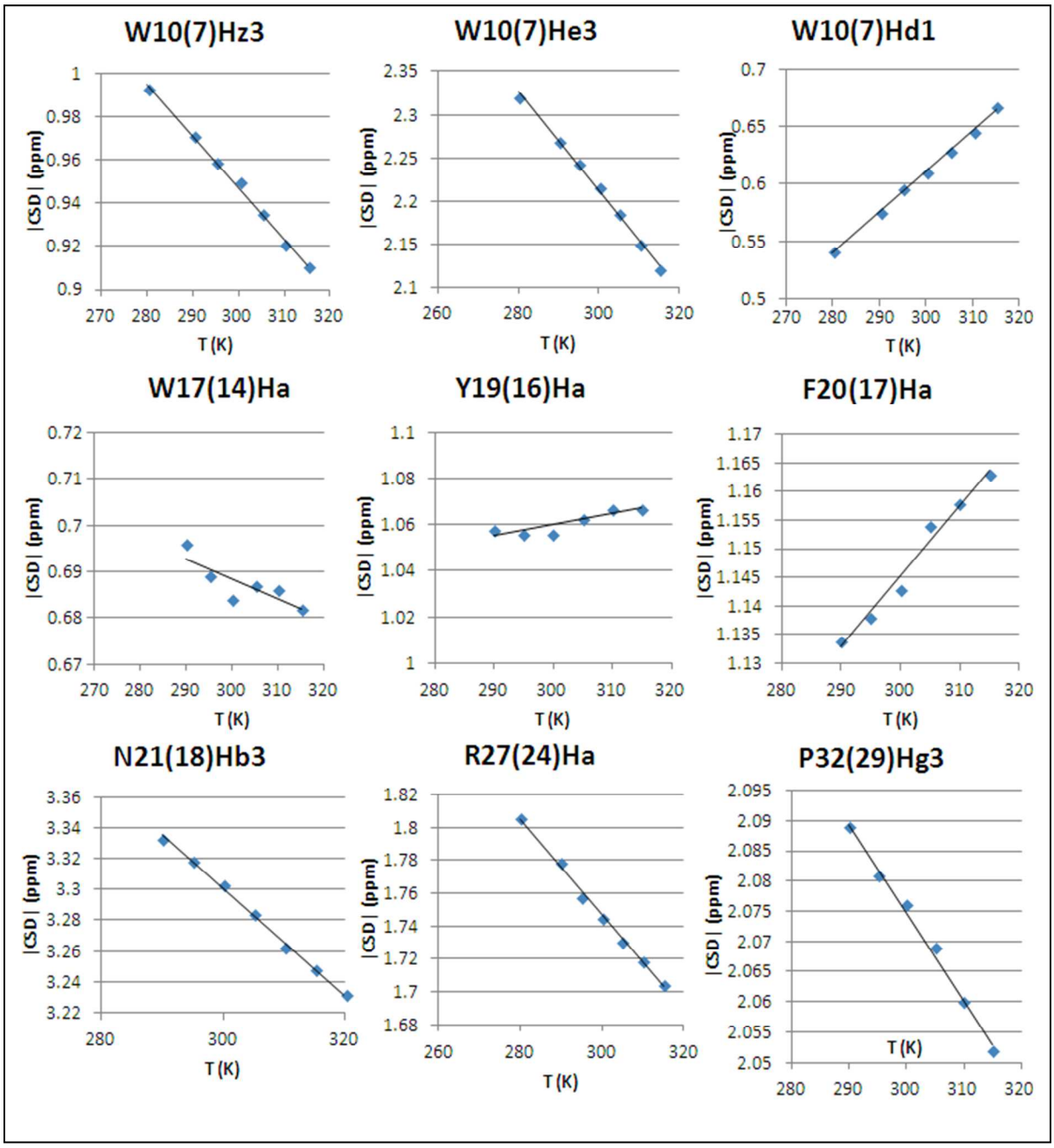

With the exception of the W17(14), Y19(*16*) and F20(*17*) Hα CSDs, which are downfield due to cross-strand interactions in the β-sheet (2), the other CSDs are negative, reflecting upfield ring-current shifts. The temperature dependence in the folded state δ values is attributed to increased fluctuation of aryl group chi values on warming.

Fig. S8. Folding dynamics data for WW **st**29 (top panel) and WW **cp**29 (lower panel) showing the points for each exchange-broadened probe employed.

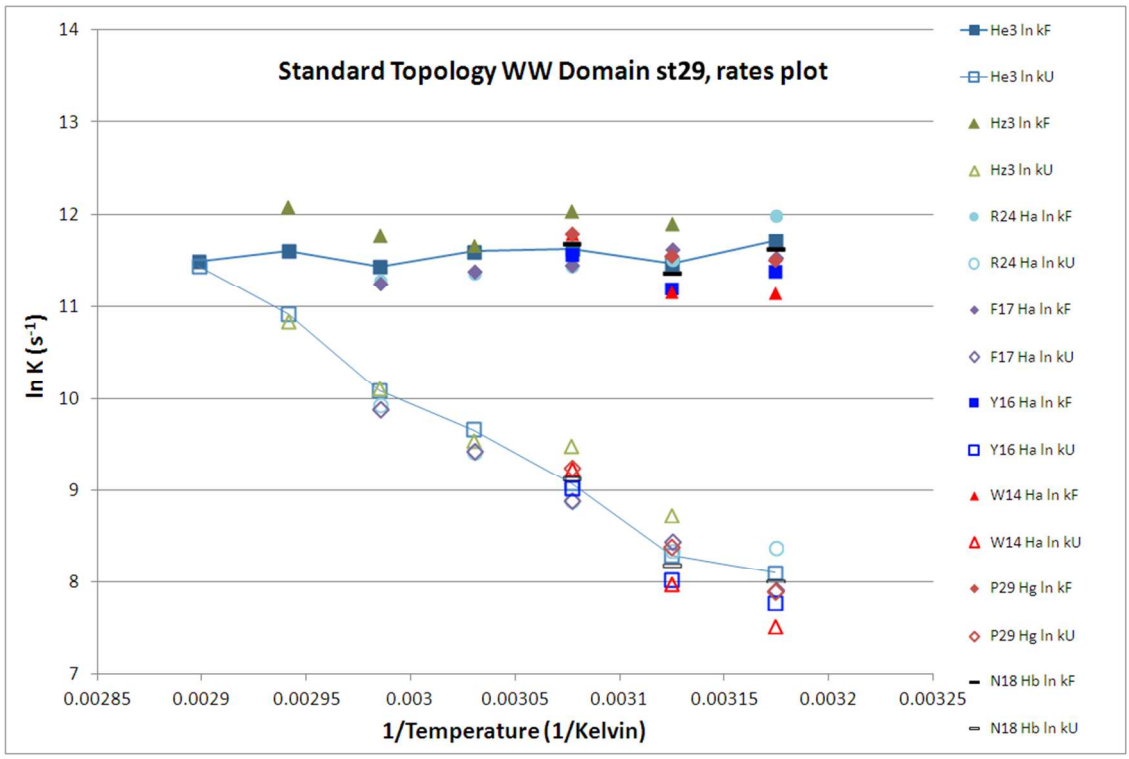

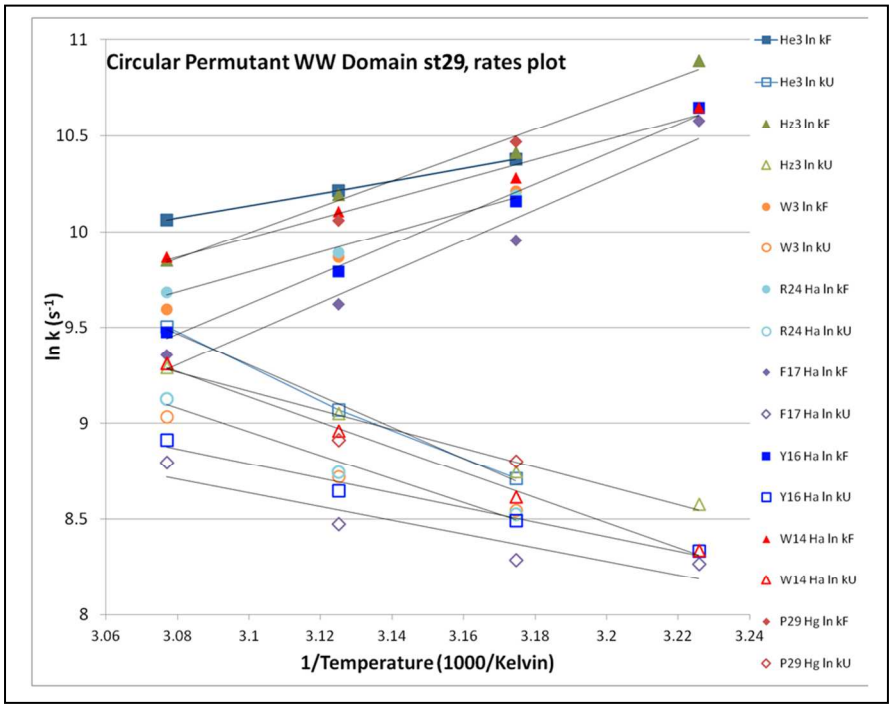

Some probes were not usable, or accessible, at all temperatures, due to either too much or too little line broadening, or direct overlap with another peak.

Although the scale employed in the lower panel appears to indicate greater variation between probes, it was actually comparable for the two species. For WW **cp**29, the largest error in ln k was ±0.24. We view the observation of essentially identical Arrhenius plot slopes as evidence for 2-state folding in this system.

Exploring an Alternative Circular Permutation Cut Point (excision of turn-2)

While circular permutation is a highly useful technique for probing folding pathways, it is not always obvious when it will prove viable. While we had great success in excising fold-nucleating turn 1, excision of less-crucial turn 2 (that is, design of a WW domain circular permutant with its termini moved to turn 2) proved more problematic. Our difficulties were likely a consequence of the smaller size and thus docking propensity of strand 3. Instead of a complete WW domain that folds via a standard 2-state mechanism, we instead observed – for all 3 attempts - a fully-folded hairpin1 and very broad lineshapes elsewhere. Evidence for a significant population (>50%) of complete WW domain was observed (*e.g.*, certain large chemical shifts, etc.) but the protein was very difficult to characterize, and solubility was poor. This and the construction of circularly permuted Pin1 variant with tunable kinetic traps will require further study.

Optimization Potential of WW st29:

We expect that WW **st**29 could fold at record-breaking speeds if known rate-enhancing mutations at the RGSG turn locus (*e.g.* [PATG]- or [ADG]-mutations) were applied to it. These constructs were expected to have Tm values well above our (NMR) temperature window, placing them outside the scope of the current study. However, these constructs could be amenable to NMR lineshape studies when combined with low-phi-value destabilizing mutations. We plan to investigate these possibilities as part of our ongoing optimization and rate characterization studies of WW **st**29 and **cp**29.

The NMR structure of WW cp29

The structure ensemble generation procedure previously used for both hairpins (1,4,5) and small proteins (6-8) was applied to 473 NOE intensities observed for WW **cp**29. The automated distance-constraint derivation, MD annealing protocols (using a CNS script), and acceptance criteria were those described previously.(5,6) The structure statistics (Table S1) and distance constraints (Table S2) appear below.

The in-house program used to convert NOE intensities to distance constraints produces constraints in the form, $d - \Delta d_{neg}$ to $d + \Delta d_{pos}$ being the allowed distance range. Our calibration and error analysis procedure yields constraints that are tighter than those used in many NOE ensemble generation procedures. In the present case, it resulted in the following average values over the full set of NOE constraints: d = 3.25 ±0.60 Å (±0.60), Δd_{neg} = 0.58 ± 0.31 Å, and Δd_{pos} = 0.52 ± 0.20 Å. The large number and relative tightness of these constraints contributed to the lower-than-expected acceptance rate of the generated ensemble (22 structures of 40) and the somewhat larger than usual average NOE violation listed in Table S1.

Chemical shift data can be found in accession number 19503 at the Biological Magnetic Resonance Bank (BMRB) at http://www.bmrb.wisc.edu/devise/peptide-cgi/html/uvd/pacu_20130923_20411/pacu_20130923_20411ps1.html.

Fig. S9: Structure of WW **cp**29 (PDB ID 3tc7, **cyan**) overlaid with wild-type WW Pin1 domain (PDB ID 2mdu, **green**).

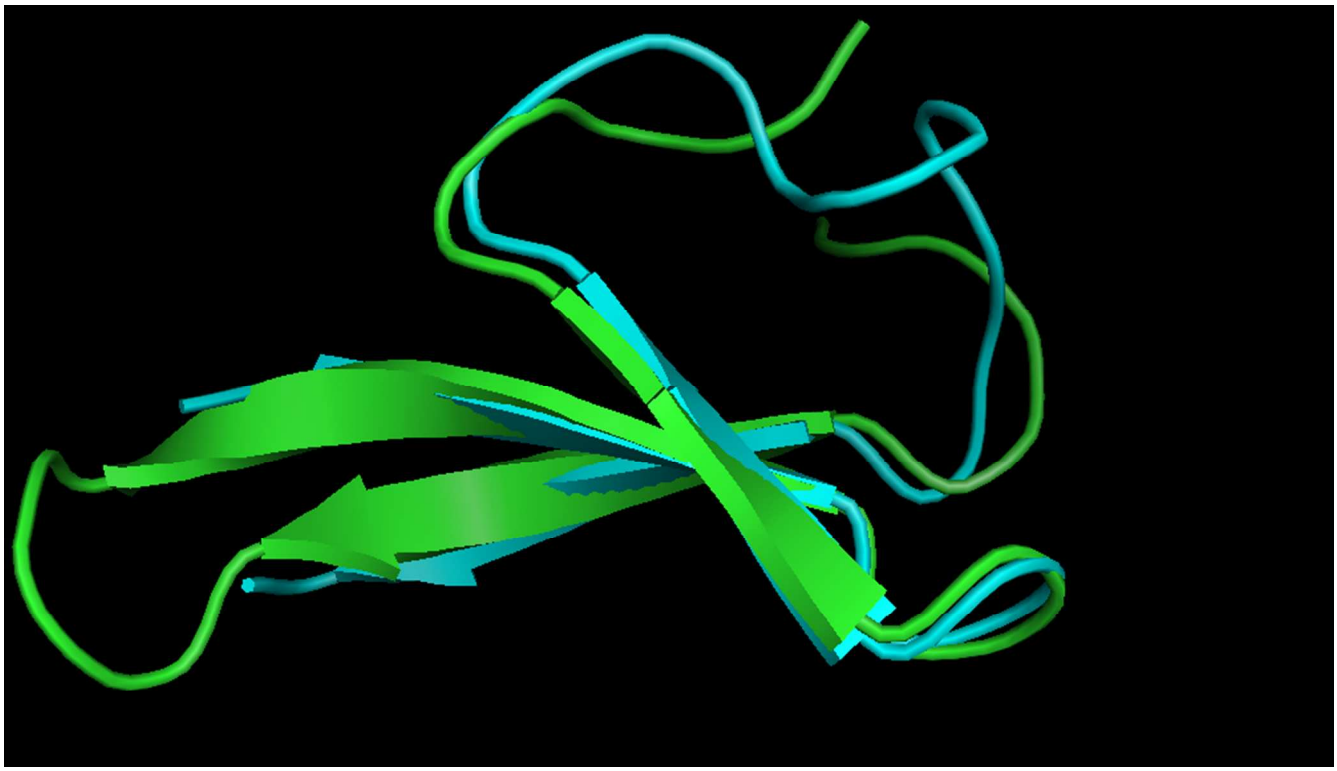

The only significant sidechain orientation difference in a shared region of sequence is highlighted: the WW **cp**29 Phe14 vs. analogous wild-type Trp29, which adopt different $\chi 1$ rotamers. (Though in our NMR ensemble, this Phe was flexible and could be found in the native rotamer in some structures.)

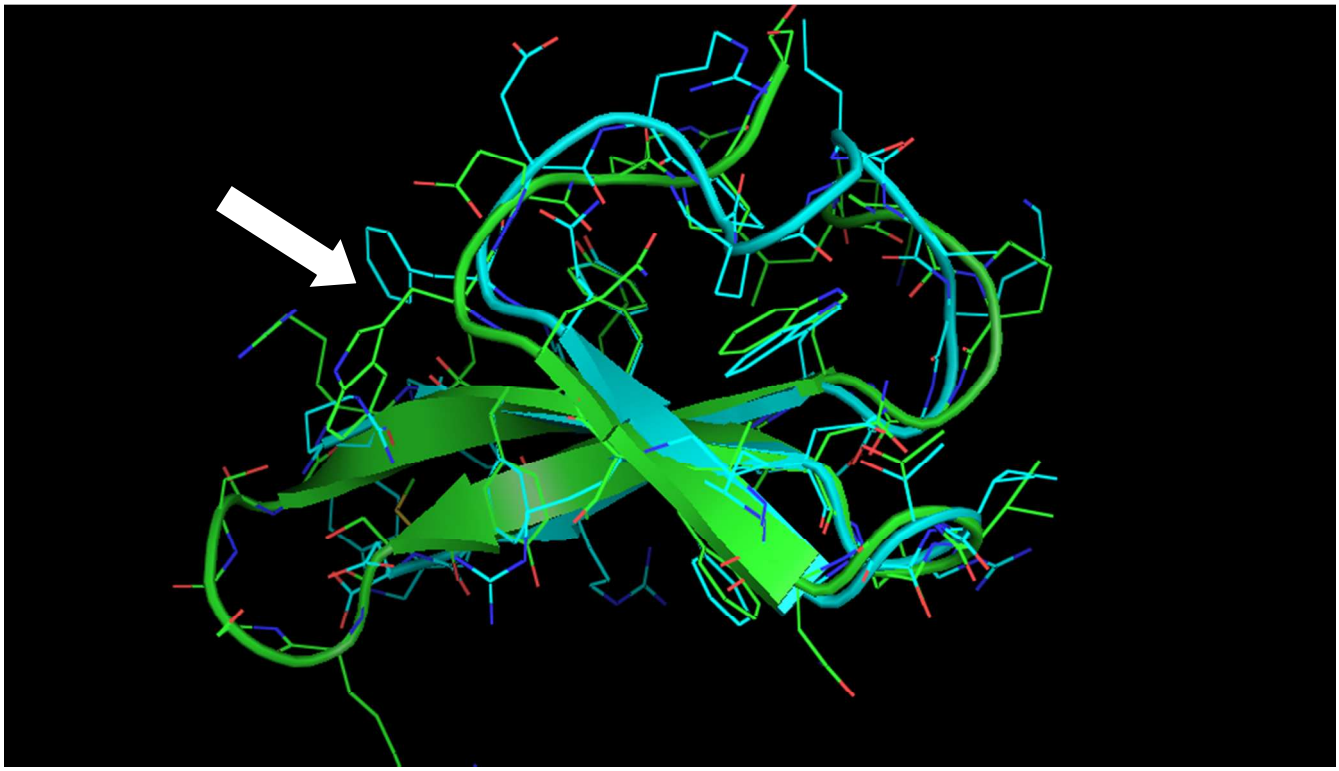

The only other points of difference are across non-shared sequence space; e.g., the connecting loops which are excised from the other constructs. The essential proline (WW **cp**29: P17, wild-type: P32), adopts a similar, but not identical, orientation between structures, and the residues beyond that (the connecting loop region of WW **cp**29, and the C-terminal residues of the wild-type) deviate significantly. Similarly, the opposite end of WW **cp**29's loop only overlays well with the N-terminal residues of the wild-type at or after residue K22 (P4 of wild-type). These loop/terminal residues were not included in the backbone heavy-atom RMSD calculation of 1.08 angstroms. The RMSD near the tighter loop of the wild-type's hairpin 1 (the beta-capped termini of WW **cp**29) is significantly better.

Because the connecting loop of WW **cp**29 cannot adopt the same orientation the very N and C terminal tails of the wild-type that it replaces, one hydrophobic packing interaction is lost: the contact between the wild-type's L2 with hydrophobic core residues W6 and Y19. Though this interaction is known to be stabilizing, it is inessential, and the N-terminal tail is flexible. The N-terminal sequence segment is not present in some NMR and crystal structures, presumably due to flexibility (e.g., PDB ID 1zr7). In our longer, hyperstable standard-topology WW domain (WW **st**34), L2 had practically no CSDs, and its NOEs to hydrophobic core residues were much weaker than expected, given its expected structure. (It was expected to be identical to wild-type, as there are no mutations in this region. All other diagnostics matched expectations from the wild-type structure; for example, the CSD diagnostics of figures S6A&B.)

Table S2. WW cp29, NMR structure ensemble statistics (22 accepted structures from 40).

Type of constraint	Number
Intraresidue	222
Sequential	101
i/i+n, n = 2-4	32
i/i+n, n ≥ 5	118
Structure statistics[a.].	r.m.s deviation
E_{vdW} (kcal/mol)	-7.3 ± 80.1
Bond violations (Å)	0.011± 0.002
Angle violations (°)	1.11 ± 0.15
Improper torsion violations (°)	0.94 ± 0.25
NOE violations (Å)	0.13 ± 0.034
Convergence within final ensemble, atomic r.m.s deviations (Å, ±s.e.):	
Pairwise over the entire ensemble	
Backbone	1.30 ± 0.72
Heavy atom	2.38 ± 0.73
Excepting the loop connecting former termini (residues 18-22)	
Backbone	0.77 ± 0.40
Heavy atom	1.87 ± 0.51

[a.] Values are mean ± standard deviation over the 22 accepted structures.

Table S3. NOE-derived distance constraints used to elucidate the WW CircMutant (cp29) structure.

range	#1	proton	#2	proton	distance (Å)	Δd_{neg} (Å)	Δd_{pos} (Å)
27	1	ha	28	hz3	3.33	0.54	0.64
27	1	ha	28	hh2	3.59	0.62	0.73
27	2	ha	29	hn	3.53	0.6	0.51
26	28	hz3	2	hd1	2.96	0.42	0.74
26	28	hz3	2	he1	3.19	0.49	0.8
26	28	hb2	2	hz3	3.34	0.54	0.64
26	28	ha	2	he3	3.35	0.54	0.65
26	28	he3	2	hz3	3.39	0.56	0.86
26	28	he3	2	he3	3.67	0.65	0.96
26	28	hb2	2	he3	3.7	0.66	0.78
26	28	he3	2	hd1	3.83	0.7	1.03
26	28	hz3	2	hn	3.95	0.73	0.89
26	29	hb2	3	he#	3.32	0.51	0.83
26	29	hb1	3	hd#	3.34	0.52	0.84
26	29	hb2	3	hd#	3.34	0.52	0.84
26	2	hz3	28	hn	3.9	0.72	0.87
26	3	hd#	29	hn	3.33	0.52	0.83
26	3	he#	29	hn	3.44	0.55	0.86
25	2	hz3	27	hn	3.83	0.7	0.83
25	2	he3	27	hn	3.84	0.7	0.84
24	26	hg2	2	he3	2.86	0.39	0.51
24	26	hg1	2	he3	3.42	0.57	0.67
24	26	hb1	2	he3	4.08	0.78	0.96
24	27	hn	3	hn	3.03	0.44	0.35
24	27	hb1	3	hz	3.38	0.55	0.65
24	27	hb1	3	he#	3.56	0.59	0.9
24	27	hb2	3	hz	3.88	0.71	0.86
24	27	hb1	3	hd#	4.02	0.74	1.09
24	27	hb2	3	hd#	4.06	0.75	1.11
23	4	ha	27	hn	3.64	0.63	0.55
23	4	hd#	27	hn	4.05	0.75	1.11
22	26	hb2	4	he#	3.15	0.46	0.78
22	26	hb2	4	hd#	3.55	0.59	0.9
22	26	hd1	4	he#	3.61	0.6	0.92
22	26	ha	4	hd#	3.66	0.62	0.94
22	26	hb1	4	he#	4.08	0.76	1.12
22	26	hg1	4	he#	4.17	0.78	1.17
21	26	ha	5	hn	3.39	0.56	0.46

20	24	he3	4	hd#	3.47	0.56	1.08
20	25	hb2	5	hd#	3.08	0.44	0.76
20	4	hb2	24	he3	2.56	0.29	0.45
20	4	hb1	24	he3	3.21	0.5	0.6
20	4	ha	24	he3	3.53	0.6	0.71
20	5	hb2	25	hn	3.49	0.59	0.49
20	5	hb1	25	hn	3.96	0.74	0.69
19	24	he3	5	hn	3.08	0.46	0.57
19	6	ha	25	hn	3.35	0.54	0.45
18	24	he3	6	hn	4.5	1.16	1.36
18	24	hh2	6	hn	4.5	1.36	1.56
18	6	hb1	24	hz3	2.67	0.33	0.47
18	6	ha	24	hn	3.08	0.46	0.37
18	6	hb2	24	hz3	3.15	0.48	0.58
18	6	hd21	24	he1	3.28	0.52	0.62
18	6	hb1	24	hh2	3.31	0.53	0.63
18	6	hb2	24	he3	3.32	0.53	0.64
18	6	hd22	24	he1	3.59	0.62	0.73
18	6	hb1	24	he3	3.65	0.64	0.75
18	6	hd21	24	he3	3.68	0.65	0.77
18	6	ha	24	he3	3.76	0.67	0.8
18	6	ha	24	hb1	3.92	0.72	0.67
18	6	hd22	24	hn	4.04	0.76	0.74
17	23	ha2	6	hd22	3.57	0.62	0.53
17	23	ha2	6	hd21	4.18	0.81	0.82
17	24	ha	7	hn	3.18	0.49	0.39
16	23	ha2	7	hn	3.85	0.7	0.64
16	23	ha1	7	hb1	4.06	0.77	0.75
15	23	ha2	8	hd1#	3.95	0.6	0.5
15	23	ha1	8	hd1#	4	0.6	0.5
15	21	hg2#	6	hd2*	3.59	0.62	0.53
13	11	hb2	24	hh2	3.87	1.01	1.15
13	11	hb2	24	hz3	3.87	1.01	1.15
13	11	hb1	24	hh2	4.02	0.96	1.13
13	11	hg1	24	hh2	4.06	0.97	1.15
13	17	hd1	4	hd#	3.6	0.6	0.92
13	17	hd2	4	hd#	3.84	0.68	1.01
13	17	hd2	4	he#	3.99	0.73	1.08
13	17	hd1	4	he#	4.03	0.74	1.1
13	17	hg2	4	hd#	4.16	0.78	1.16
13	1	hg2	14	hd#	3.99	0.73	1.08
13	1	hg2	14	he#	4.21	0.79	1.19

13	1	hg1	14	he#	4.47	0.88	1.34
12	16	ha	4	he#	3.16	0.46	0.79
12	4	he#	16	hn	3.53	0.58	0.89
11	13	hg2	24	hh2	4.6	0.94	1.31
11	14	ha	3	hb1	3.35	0.54	0.44
11	14	ha	3	hd#	3.65	0.62	0.94
11	14	ha	3	hb2	4	0.75	0.72
11	15	ha	4	he#	3.98	0.72	1.07
11	15	ha	4	hd#	6.46	1.51	4.17
11	24	hz3	13	hn	3.22	0.5	0.61
11	3	hb1	14	hd#	3.01	0.42	0.75
11	3	hb2	14	hd#	3.35	0.52	0.84
10	14	ha	4	hd#	3.19	0.47	0.79
10	14	ha	4	hn	3.41	0.56	0.46
10	3	hd#	13	hn	3.6	0.6	0.92
9	12	hb2	3	hd#	2.75	0.33	0.69
9	12	hg2	3	he#	3.01	0.42	0.75
9	12	hg1	3	he#	3.34	0.52	0.83
9	12	hg2	3	hd#	3.62	0.61	0.93
9	12	hg1	3	hd#	4.03	0.74	1.1
9	4	hn	13	hn	3.15	0.48	0.38
9	4	hb1	13	hn	4.18	0.81	0.82
8	5	ha	13	hn	3.7	0.65	0.58
7	12	hb2	5	hd#	2.62	0.29	0.67
7	12	ha	5	hd#	2.75	0.33	0.69
7	12	hb2	5	he#	4.17	0.78	1.16
7	12	hg1	5	he#	4.46	0.87	1.34
7	17	ha	24	hd1	4	1.2	1.5
7	17	hb1	24	hd1	4.5	1.2	1.5
7	17	hb2	24	he1	3.48	0.58	0.69
7	5	ha	12	ha	3.04	0.45	0.36
6	12	ha	6	hn	3.53	0.6	0.51
6	18	hb2	12	hn	3.43	0.57	0.47
5	10	ha1	5	he#	3.13	0.45	0.78
5	10	ha1	5	hz	3.19	0.49	0.6
5	10	ha2	5	hz	3.52	0.6	0.7
5	10	ha2	5	he#	3.62	0.61	0.93
5	11	hn	6	hn	2.9	0.7	0.62
4	6	hb1	10	hn	3.51	0.59	0.5
4	17	ha	13	he2*	3.13	0.48	0.38
4	17	ha	13	he2*	2.64	0.32	0.27
4	17	hd1	13	he2*	3.75	0.67	0.6

3	17	hd1	20	hn	3.83	0.7	0.63
3	21	ha	24	hd1	2.66	0.33	0.47
3	21	hb	24	hd1	3.06	0.45	0.56
3	21	hb	24	he1	3.19	0.49	0.6
3	21	ha	24	he1	3.37	0.55	0.65
3	24	hd1	21	hn	3.62	0.63	0.74
3	6	hb1	9	hn	3.8	0.69	0.62
3	7	ha	10	hn	3.41	0.56	0.46
3	21	hg2#	24	hd1	2.72	0.35	0.28
3	21	hg2#	24	he1	2.67	0.33	0.27
2	11	hn	9	hn	3.49	0.59	0.49
2	13	hb1	15	hn	3.14	0.48	0.38
2	13	ha	15	hn	3.41	0.56	0.46
2	13	hg1	15	hn	3.61	0.63	0.54
2	13	hg2	15	hn	3.66	0.64	0.56
2	22	ha	24	hn	3.01	0.44	0.35
2	7	ha	5	he#	2.43	0.23	0.64
2	7	ha	5	hz	2.97	0.42	0.54
2	7	ha	5	hd#	3.21	0.48	0.8
2	7	hb2	5	he#	3.34	0.52	0.84
2	8	hn	10	hn	3.15	0.48	0.39
2	9	hb	11	hn	3.56	0.61	0.52
2	9	hg1	11	hn	3.76	0.67	0.6
2	9	ha	11	hn	3.98	0.74	0.71
2	13	he2*	15	hn	3.83	0.7	0.64
2	15	hb2	13	he2*	3.25	0.51	0.41
2	15	hb2	13	he2*	3.9	0.72	0.67
2	9	hg2#	11	hn	3.84	0.7	0.64
1	10	ha1	11	hn	3.28	0.52	0.42
1	10	ha2	11	hn	4.03	0.76	0.73
1	10	ha1	9	hn	4.06	0.77	0.75
1	11	hn	10	hn	2.58	0.3	0.25
1	11	ha	12	hn	2.14	0.16	0.18
1	11	hb2	12	hn	4	0.95	0.92
1	12	ha	13	hn	2.24	0.19	0.2
1	12	hb2	13	hn	2.84	0.38	0.31
1	12	hn	13	hn	3.96	0.74	0.7
1	13	ha	14	hn	2.22	0.19	0.19
1	13	hb1	14	hn	2.97	0.42	0.34
1	13	hg2	14	hn	3.6	0.62	0.53
1	13	hg1	14	hn	4.13	0.79	0.79
1	14	hb1	15	hn	3.13	0.47	0.38

1	14	hb2	15	hn	3.38	0.55	0.45
1	14	ha	15	hn	3.45	0.58	0.48
1	14	hd#	15	hn	4.27	0.81	1.22
1	15	hn	14	hn	2.55	0.29	0.25
1	15	ha	16	hn	1.92	0.19	0.26
1	15	hb1	16	hn	2.78	0.36	0.29
1	15	hb2	16	hn	2.87	0.39	0.31
1	15	hn	16	hn	3.68	0.65	0.57
1	16	ha	17	hd1	2.36	0.23	0.22
1	16	ha	17	hd2	2.53	0.28	0.24
1	17	ha	18	hn	2.1	0.15	0.18
1	17	hb1	18	hn	3.29	0.52	0.43
1	17	hb2	18	hn	3.35	0.55	0.45
1	18	ha	19	hn	2.42	0.25	0.23
1	18	hb2	19	hn	3.52	0.8	0.71
1	1	ha	2	hn	2.23	0.19	0.2
1	1	hg2	2	hn	3.09	0.46	0.37
1	1	ha	2	hd1	3.55	0.61	0.71
1	1	hb2	2	hn	3.62	0.63	0.54
1	1	hg1	2	hn	3.64	0.64	0.55
1	20	hb2	19	hn	3.53	0.6	0.51
1	20	ha	21	hn	2.28	0.21	0.2
1	20	hb2	21	hn	3.74	0.67	0.59
1	20	hd2#	21	hn	4.72	0.87	0.82
1	21	hn	20	hn	3.41	0.56	0.46
1	21	ha	22	hn	2.09	0.15	0.18
1	21	hb	22	hn	2.96	0.42	0.33
1	21	hn	22	hn	3.07	0.96	0.86
1	22	ha	23	hn	2.39	0.24	0.22
1	22	hb2	23	hn	3.2	0.5	0.4
1	22	hn	23	hn	3.85	0.7	0.64
1	23	ha2	24	hn	3.28	0.52	0.42
1	23	ha1	24	hn	3.46	0.58	0.48
1	24	hn	23	hn	2.9	0.4	0.32
1	24	ha	25	hn	2.25	0.19	0.2
1	24	he3	25	hn	3.03	0.44	0.55
1	24	hb1	25	hn	3.32	0.54	0.44
1	24	hb2	25	hn	3.81	0.69	0.62
1	25	ha	26	hn	2.09	0.15	0.18
1	25	hb1	26	hn	3.42	0.57	0.47
1	25	hg1	26	hn	3.67	0.65	0.56
1	26	ha	27	hn	2.15	0.16	0.18

1	26	hg2	27	hn	3.76	0.67	0.6
1	26	hg1	27	hn	3.83	0.7	0.63
1	27	ha	28	hn	2.26	0.2	0.2
1	27	hb2	28	hn	2.95	0.42	0.33
1	27	hg2	28	hn	3.47	0.58	0.48
1	27	hb1	28	hn	3.66	0.64	0.56
1	27	hg1	28	hn	3.77	0.68	0.6
1	28	ha	29	hn	2.18	0.17	0.19
1	28	hb2	29	hn	3.71	0.66	0.58
1	28	hb1	29	hn	3.87	0.71	0.65
1	2	ha	3	hn	2.23	0.19	0.2
1	2	he3	3	hn	3.16	0.48	0.59
1	2	hb1	3	hn	3.17	0.49	0.39
1	2	hb2	3	hn	3.38	0.55	0.46
1	3	hb2	4	hn	2.63	0.32	0.26
1	3	hb1	4	hn	3.18	0.49	0.39
1	3	hb1	4	hd#	3.28	0.5	0.82
1	3	hd#	4	hn	3.29	0.5	0.82
1	3	hb1	4	he#	3.68	0.63	0.95
1	3	ha	4	hn	2.5	0.7	1.5
1	4	ha	5	hn	2.32	0.22	0.21
1	4	hb2	5	hn	3.46	0.58	0.48
1	4	hd#	5	hn	3.81	0.67	1
1	4	hb1	5	hn	3.97	0.74	0.7
1	5	ha	6	hn	2.27	0.2	0.2
1	5	hd#	6	hn	2.74	0.33	0.69
1	5	hb2	6	hn	4.16	0.8	0.8
1	6	ha	7	hn	2.08	0.14	0.18
1	7	hb1	8	hn	3.32	0.53	0.44
1	8	hn	7	hn	2.62	0.31	0.26
1	8	hb	9	hn	2.61	0.31	0.26
1	8	ha	9	hn	3.38	0.55	0.46
1	8	hg2#	9	hn	3.73	0.56	0.45
1	8	hg12	9	hn	4.2	0.81	0.83
1	9	hn	10	hn	2.35	0.23	0.21
1	9	ha	10	hn	2.88	0.39	0.31
1	9	hb	10	hn	3.51	0.6	0.5
1	9	hn	8	hn	2.51	0.28	0.24
1	9	ha	8	hg2#	3.9	0.61	0.5
1	21	hg2#	20	hn	3.69	0.65	0.57
1	21	hg2#	22	hn	2.76	0.36	0.29
1	9	hg2#	10	hn	3.34	0.54	0.44

1	9	hg2#	8	hb	3.42	0.57	0.47
1	9	hg2#	8	hn	3.6	0.62	0.53
1	9	hg2#	8	hg2#	2.18	0.17	0.19
0	10	ha1	10	hn	2.39	0.24	0.22
0	10	ha2	10	hn	2.84	0.38	0.31
0	11	hb2	11	hn	2.65	0.52	0.47
0	11	hb1	11	hn	2.89	0.6	0.52
0	11	ha	11	hn	2.91	0.41	0.32
0	11	hg2	11	hn	2.91	0.6	0.52
0	11	ha	11	hb1	3.02	0.64	0.55
0	11	hg1	11	hn	3.05	0.65	0.56
0	11	ha	11	hd2	3.13	0.68	0.58
0	11	ha	11	hg1	3.5	0.79	0.7
0	11	hd2	11	hn	3.51	0.79	0.7
0	11	ha	11	hg2	3.59	0.82	0.73
0	12	hb1	12	hn	2.89	0.4	0.32
0	12	hb2	12	ha	3.02	0.44	0.35
0	12	hb2	12	hn	3.07	0.46	0.36
0	12	ha	12	hn	3.15	0.48	0.38
0	12	hg2	12	hn	3.19	0.49	0.4
0	12	hd1	12	he	3.31	0.53	0.43
0	12	hd2	12	he	3.34	0.54	0.44
0	12	hg1	12	hn	3.57	0.61	0.52
0	12	hb2	12	he	3.64	0.64	0.55
0	12	hg1	12	he	3.69	0.65	0.57
0	13	ha	13	hn	2.77	0.36	0.29
0	13	hb2	13	hn	3.01	0.44	0.35
0	13	hb1	13	hn	3.3	0.53	0.43
0	13	hg1	13	hn	3.38	0.55	0.46
0	13	hg2	13	hn	3.76	0.67	0.6
0	14	hd#	14	he#	1.97	0.07	1.02
0	14	ha	14	hd#	2.39	0.22	0.63
0	14	hb1	14	hd#	2.55	0.27	0.66
0	14	hb2	14	hd#	2.61	0.29	0.67
0	14	hd#	14	hz	2.74	0.33	0.9
0	14	hb1	14	hn	2.78	0.36	0.29
0	14	ha	14	hn	2.85	0.38	0.31
0	14	ha	14	hb1	3.03	0.44	0.35
0	14	hb2	14	hn	3.09	0.46	0.37
0	14	hd#	14	hn	3.19	0.47	0.79
0	14	ha	14	hb2	3.32	0.54	0.44
0	14	ha	14	he#	3.4	0.54	0.85

0	14	hb2	14	he#	4.06	0.75	1.11
0	15	ha	15	hb2	2.45	0.26	0.23
0	15	hb1	15	hn	2.47	0.27	0.23
0	15	hb2	15	hn	2.51	0.28	0.24
0	15	ha	15	hn	2.6	0.31	0.26
0	15	hg1	15	hn	3.45	0.58	0.48
0	15	hg2	15	hn	3.48	0.59	0.49
0	16	hb2	16	hn	2.19	0.18	0.19
0	16	hb1	16	hn	2.23	0.19	0.2
0	16	ha	16	hn	2.78	0.36	0.29
0	16	hg2	16	hn	3.51	0.6	0.5
0	16	ha	16	hg2	3.59	0.62	0.53
0	17	ha	17	hb1	2.58	0.3	0.25
0	17	ha	17	hb2	2.87	0.39	0.31
0	18	he2	18	hd2	2.64	0.52	0.47
0	18	hb1	18	hn	2.76	0.56	0.49
0	18	ha	18	hn	2.78	0.56	0.49
0	18	ha	18	hb2	3.06	0.65	0.56
0	18	hb2	18	hn	3.18	0.69	0.59
0	18	ha	18	hb1	3.35	0.74	0.64
0	18	hg2	18	hn	3.5	0.59	0.5
0	18	ha	18	hg2	3.77	0.88	0.81
0	18	hg1	18	hn	3.92	0.93	0.88
0	18	ha	18	hg1	4.59	1.14	1.31
0	1	ha	1	hg2	2.95	0.42	0.33
0	1	ha	1	hg1	3.37	0.55	0.45
0	1	ha	1	hb2	3.45	0.58	0.48
0	20	ha	20	hb2	2.53	0.28	0.24
0	20	hb2	20	hn	2.65	0.32	0.27
0	20	ha	20	hn	3.05	0.65	0.56
0	20	ha	20	hd2#	3.1	0.36	0.3
0	20	hg	20	hn	3.16	0.48	0.39
0	20	ha	20	hg	3.23	0.51	0.41
0	20	ha	20	hd1#	3.78	0.58	0.46
0	20	hd1#	20	hn	4.51	0.81	0.72
0	20	hd2#	20	hn	4.84	0.91	0.88
0	21	ha	21	hn	2.65	0.32	0.27
0	21	ha	21	hb	2.85	0.39	0.31
0	21	hb	21	hn	2.89	0.4	0.32
0	22	hb2	22	hn	2.36	0.5	0.5
0	22	hb2	22	hn	2.36	0.5	0.5
0	22	ha	22	hn	2.4	0.54	0.52

0	22 hd2	22 hn	3.64	0.64	0.55
0	22 hg1	22 hn	3.65	0.64	0.56
0	22 hg2	22 hn	3.77	0.68	0.6
0	23 ha1	23 hn	2.95	0.42	0.33
0	23 ha2	23 hn	3.26	0.52	0.42
0	24 hb2	24 hn	2.48	0.27	0.24
0	24 hb1	24 he3	2.69	0.34	0.48
0	24 hb2	24 hd1	2.7	0.34	0.48
0	24 hd1	24 hn	2.83	0.38	0.5
0	24 ha	24 he3	2.85	0.39	0.51
0	24 hb1	24 hn	2.94	0.41	0.33
0	24 hb1	24 hd1	2.97	0.42	0.54
0	24 ha	24 hn	2.98	0.43	0.34
0	24 hb2	24 he3	3.55	0.61	0.72
0	25 ha	25 hn	2.99	0.43	0.34
0	25 hb2	25 hn	3.49	0.59	0.49
0	25 hb1	25 hn	3.78	0.68	0.61
0	25 hg1	25 hn	4.29	0.84	0.89
0	26 hb1	26 hn	2.85	0.39	0.31
0	26 hb2	26 hn	2.89	0.4	0.32
0	26 ha	26 hn	2.98	0.43	0.34
0	26 ha	26 hb2	3.41	0.56	0.46
0	26 ha	26 hb1	3.59	0.62	0.53
0	26 he1	26 hd1	3.62	0.63	0.54
0	26 ha	26 hg1	3.72	0.66	0.59
0	26 he2	26 hd2	3.94	0.73	0.69
0	26 hg1	26 hn	3.94	0.73	0.68
0	26 ha	26 hg2	4.45	0.89	1
0	27 hb1	27 hg1	2.72	0.34	0.28
0	27 hb1	27 hg2	2.85	0.39	0.31
0	27 ha	27 hb2	2.86	0.39	0.31
0	27 ha	27 hn	2.96	0.42	0.33
0	27 ha	27 hg2	3.06	0.45	0.36
0	27 ha	27 hg1	3.14	0.48	0.38
0	27 hg2	27 he	3.16	0.48	0.39
0	27 hd1	27 he	3.2	0.5	0.4
0	27 hg1	27 he	3.22	0.5	0.41
0	27 hb1	27 hn	3.3	0.53	0.43
0	27 hb2	27 hn	3.33	0.54	0.44
0	27 hd2	27 hb1	3.74	0.67	0.59
0	27 hd1	27 hb1	3.77	0.68	0.61
0	27 ha	27 hb1	3.82	0.69	0.63

0	27	hg1	27	hn	4.01	0.75	0.72
0	28	he1	28	hd1	1.93	0.1	0.56
0	28	hz3	28	hh2	2.12	0.15	0.58
0	28	hb1	28	hd1	2.45	0.26	0.43
0	28	he3	28	hz3	2.52	0.28	0.64
0	28	hb1	28	hn	2.71	0.34	0.28
0	28	hb2	28	hd1	2.81	0.37	0.5
0	28	hb2	28	hn	2.91	0.4	0.32
0	28	ha	28	hn	3.01	0.44	0.35
0	28	he3	28	hh2	3.43	0.57	0.87
0	28	hb1	28	he1	4.06	0.77	0.95
0	29	ha	29	hn	2.89	0.4	0.32
0	29	hb2	29	hn	3.43	0.57	0.47
0	29	hb1	29	hn	3.49	0.59	0.49
0	2	hz3	2	hh2	1.97	0.11	0.56
0	2	he1	2	hd1	2.01	0.12	0.57
0	2	hh2	2	hz2	2.13	0.16	0.58
0	2	hb2	2	hd1	2.57	0.3	0.45
0	2	hz3	2	he3	2.64	0.32	0.67
0	2	ha	2	he3	2.68	0.33	0.47
0	2	hb2	2	hn	2.81	0.37	0.3
0	2	hb1	2	hd1	2.9	0.4	0.52
0	2	hb1	2	he3	3.08	0.46	0.56
0	2	hd1	2	hn	3.11	0.47	0.57
0	2	hb1	2	hn	3.13	0.47	0.38
0	2	ha	2	hn	3.19	0.49	0.4
0	2	hb2	2	he3	3.33	0.54	0.64
0	2	he3	2	hh2	3.45	0.58	0.88
0	3	he#	3	hz	1.87	0.06	0.77
0	3	he#	3	hd#	1.95	0.06	1.02
0	3	hb2	3	hd#	2.49	0.25	0.65
0	3	hb1	3	hd#	2.49	0.25	0.65
0	3	hd#	3	hn	3	0.41	0.75
0	3	ha	3	hd#	3.1	0.44	0.77
0	3	ha	3	hn	3.15	0.48	0.38
0	3	he#	3	hn	4.01	0.73	1.09
0	3	hb1	3	hn	4.16	0.8	0.81
0	4	hb2	4	hd#	2.62	0.29	0.67
0	4	hb1	4	hd#	2.7	0.32	0.68
0	4	hb1	4	hn	2.74	0.35	0.28
0	4	hd#	4	hn	2.83	0.36	0.71
0	4	ha	4	hd#	3.04	0.42	0.75

0	4	hb2	4	he#	3.35	0.52	0.84
0	4	hb2	4	hn	3.37	0.55	0.45
0	4	ha	4	hn	3.62	0.63	0.54
0	4	hb1	4	he#	3.78	0.66	0.98
0	5	hd#	5	he#	1.95	0.06	1.02
0	5	hb2	5	hd#	2.33	0.2	0.62
0	5	hb1	5	hd#	2.46	0.24	0.64
0	5	ha	5	hd#	2.57	0.28	0.66
0	5	hd#	5	hz	2.66	0.3	0.88
0	5	hb1	5	hn	2.89	0.4	0.32
0	5	hb2	5	hn	3.21	0.5	0.4
0	5	ha	5	hn	3.25	0.51	0.41
0	5	hd#	5	hn	3.78	0.66	0.99
0	6	ha	6	hn	2.44	0.46	0.43
0	6	hb2	6	hn	2.78	0.36	0.29
0	6	hb1	6	hn	2.94	0.41	0.33
0	6	hd21	6	hb2	3.2	0.5	0.4
0	6	ha	6	hb2	3.24	0.51	0.41
0	6	hb2	6	hd22	3.33	0.54	0.44
0	6	ha	6	hb1	3.59	0.62	0.53
0	6	hd21	6	hb1	3.74	0.67	0.59
0	7	hb1	7	hn	2.33	0.22	0.21
0	7	ha	7	hb1	2.5	0.27	0.24
0	7	ha	7	hb2	2.5	0.27	0.24
0	7	ha	7	hn	2.66	0.33	0.27
0	7	hg1	7	hn	3	0.43	0.35
0	7	hg2	7	hn	3.06	0.45	0.36
0	7	ha	7	hg2	3.2	0.5	0.4
0	7	hd1	7	hb1	3.3	0.53	0.43
0	7	hd1	7	hg1	3.33	0.54	0.44
0	7	ha	7	hg1	3.46	0.58	0.48
0	7	hd2	7	he	3.47	0.58	0.49
0	7	hd1	7	he	3.78	0.68	0.61
0	7	hd2	7	hg2	3.83	0.7	0.63
0	7	hb1	7	he	3.86	0.71	0.65
0	8	hb	8	hn	2.47	0.26	0.23
0	8	ha	8	hn	2.8	0.37	0.3
0	8	ha	8	hg2#	2.83	0.28	0.26
0	8	hg12	8	hn	3.02	0.44	0.35
0	8	hg11	8	hn	3.23	0.51	0.41
0	8	ha	8	hg12	3.33	0.54	0.44
0	8	ha	8	hd1#	3.41	0.46	0.37

0	8	ha	8	hb	3.69	0.65	0.57
0	8	hg2#	8	hn	3.86	0.6	0.48
0	8	hd1#	8	hn	4.06	0.67	0.55
0	9	ha	9	hn	3.28	0.52	0.42
0	9	hb	9	hn	3.75	0.67	0.6
0	9	hg1	9	hn	4.2	0.81	0.83
0	13	hb2	13	he2*	3.13	0.48	0.38
0	13	hg1	13	he2*	2.71	0.34	0.28
0	13	hg1	13	he2*	3.34	0.54	0.44
0	13	hg2	13	he2*	3.39	0.56	0.46
0	21	hg2#	21	hn	2.39	0.24	0.22
0	21	ha	21	hg2#	2.3	0.21	0.21
0	9	hg2#	9	hn	2.49	0.27	0.24
0	9	ha	9	hg2#	2.13	0.16	0.18
0	9	hb	9	hg2#	2.1	0.15	0.18

Supporting References

1. Eidenschink, L. A.; Kier, B. L.; Huggins, K. N. L.; Andersen, N. H. *Prot. Struct. Funct. Bioinf.* **2009**, *75*, 308.

2. Fesinmeyer, R. M.; Hudson, F. M.; Olsen, K. A.; White, G. W. N.; Euser, A., Andersen, N. H. *J. Biomol. NMR* **2005**, *33*, 213.

3. Shu, I.; Scian, M.; Stewart, J. M.; Kier, B. L.; Andersen, N. H. *J. BioMol. NMR* **2013***, 56*, 313.

4. Kier, B. L.; Shu, I.; Eidenschink, L. A.; Andersen NH. *Proc. Natl. Acad. Sci. USA* **2010**, *107*, 10466.

5. Andersen, N. H.; Olsen, K. A.; Fesinmeyer, R. M.; Tan, X.; Hudson, F. M.; Eidenschink, L. A.; Farazi, S. R. *J. Am. Chem. Soc.* **2006**, *128*, 6101.

6. Williams, D. V.; Byrne, A.; Stewart, J. M.; Andersen, N. H. *Biochemistry* **2011**, *50*, 1143.

7. Barua, B.; Lin, J. C.; Williams, D. V.; Neidigh, J. W.; Kummler, P.; Andersen, N. H. *PEDS* **2008***, 21*, 171.

8. Scian, M.; Lin, J. C., Le Trong, I.; Makhatadze, G. I.; Stenkamp, R. E.; Andersen, N. H. *Proc. Natl. Acad. Sci. USA* **2012**, *109*, 12521.